

## euces: european cryogenic engineering software tool

Armin Isselhorst, Thermal & Functional Propulsion Engineering, TE52  
 EADS-SPACE Transportation, P.O. Box 286156, 28361 Bremen, Germany

The **euces** project was initiated to be prepared for the future role of EADS as stage system prime for stage and launcher developments. Launcher stages for NGLV (New Generation Launch Vehicles) need to meet ambitious mission and operational demands. The paper presents a brief overview of the EcosimPro S/W kernel and as a 1<sup>st</sup> example for **euces** application range a simplified functional model of the acceptance test bench for the 2-stage regulator of the Ariane 5 EPS (Étage Propulsive Stockable) upper stage w.r.t. physical model formulation of its incorporated components, its "schematic" and data initialisation in EcoDiagram as well as simulation results obtained in EcoMonitor. These results will be compared to acceptance test data performed at AL (Air Liquide).

### Nomenclature

#### Latin letters

$A$	= cross section	$m^2$
$c_D$	= discharge coefficient	
$c_p$	= specific heat capacity at const. pressure	J/kg/K
$c_{sp}$	= spring stiffness	N/m
$d$	= diameter	m
$D$	= diameter	m
$e$	= specific total energy	J/kg
$E$	= total energy	J
$f$	= friction factor	
$F$	= force	N
$g$	= gravity acceleration	$m/s^2$
$h$	= height	m
$h$	= specific enthalpy	J/kg
$H$	= height	m
$l$	= length	m
$L$	= length	m
$m$	= mass	kg
$\dot{m}$	= mass flow rate	kg/s
$Nu$	= Nusselt number	
$P$	= pressure	Pa
$Pr$	= Prandtl number	
$r$	= radius	m
$\dot{q}$	= heat flux density	$W/m^2$
$\dot{Q}$	= heat flux	W
$R$	= radius	m
$R$	= specific gas constant	J/kg/K
$Re$	= Reynolds number	
$S$	= surface	$m^2$
$t$	= time	s
$T$	= absolute temperature	K
$u$	= specific internal energy	J/kg

$v$	= specific volume	$\text{m}^3/\text{kg}$
$V$	= volume	$\text{m}^3$
$w$	= flow velocity	$\text{m/s}$
$x$	= poppet displacement	$\text{m}$
$\dot{x}$	= poppet velocity	$\text{m/s}$
$\ddot{x}$	= poppet acceleration	$\text{m/s}^2$
$Z$	= compressibility factor for state equation	

#### Greek letters

$\alpha$	= angle	$^\circ, \text{rad}$
$\beta$	= contraction coefficient	
$\gamma$	= heat transfer coefficient	$\text{W/m}^2/\text{K}$
$\delta$	= isothermal compressibility	$1/\text{K}$
$d$	= expulsion thickness	$\text{m}$
$\Delta$	= difference	
$k$	= adiabatic exponent	
$h$	= dynamic viscosity	$\text{Pa s}$
$l$	= heat conductivity	$\text{W/m/K}$
$m$	= sliding friction	$\text{Ns/m}$
$n$	= kinematic viscosity	$\text{m}^2/\text{s}$
$x$	= pipe friction value	
$V$	= loss coefficient	
$Y$	= void fraction	
$\rho$	= density	$\text{kg/m}^3$
$j$	= velocity coefficient	
$p$	= ratio of circumference to diameter of circle	
$q$	= angle	$^\circ, \text{rad}$
$J$	= temperature in degree Celsius	$^\circ\text{C}$
$\Psi$	= stream function	

#### Indices

$\infty$	infinity
$a$	outlet
$bel$	bellow
$const$	constant
$crit$	critical pressure ratio
$D$	discharge
$e$	jet
$HP$	high pressure
$i$	inlet
$lam$	laminar
$lim$	limes
$LP$	low pressure
$m$	intermediate
$max$	maximum
$pist$	piston
$pop$	poppet
$pre$	pre-stress
$sh$	poppet shaft
$s$	solid
$sp$	spring
$th$	theoretical
$turb$	turbulent
$w$	wall

## I. Introduction

**T**HE **euces** project was initiated to be prepared for the future role of EADS as stage system prime for stage and launcher developments. Launcher stages for NGLV (New Generation Launch Vehicles) need to meet ambitious mission and operational demands. Major technical challenges are driven by the versatility e.g. long orbit coasting under low g conditions coupled with multiple re-start of the main engine. RLV (Reusable Launch Vehicles) conceptual studies are driven by various geometrical architecture possibilities with various kinds of installed propulsion systems i.e. gas generator or stage combustion cycles for rocket propulsion system with its multiple design variations e.g. (un)winged, vertical or horizontal take-off and landing.

The project is specifically dedicated to the development of launcher system and stage analysis software for the simulation of functional behaviour of launcher stages during its ground and flight phases. It incorporates the time-dependent simulation of the complete propulsion system including all its interacting components.

In more detail, it comprises the evaluation of pressurant and propellant consumption, mass flows in the piping system, pressure regulation, feed-line chill-down in case of cryogenic propellants, engine characteristic parameters, ignitions and shut-down of engine and the sequence evaluation for the main propulsion or attitude control system. The categories involved are heat and mass transfer, thermodynamics, hydraulics, pneumatics, phase change of propellants, combustion, control and thermal aspects, as well as specific component design for tanks, valves, regulators, turbo machinery and rocket engines as a central role.

Comparison (Ref. 7) for existing in-house S/W (Software) tools showed a poor potential of adoptability to future functional stage propulsion analysis enhancements and demands. As S/W kernel EcosimPro was chosen for the **euces** project after comparison and assessment of COTS (Commercial of the Shelf) S/W w.r.t. requirement demands.

For the relevant hardware component formulation the existing hardware design of Ariane 5 upper stages was taken into consideration i.e. all hardware components have to be mathematically modelled adequately having an impact on the system simulation results.

**euces** is based on EcosimPro (Ref. 6) which was initially an ESA funded S/W tool developed by EAI (Empresarios Agrupados International, Madrid) for dynamic modelling and simulation for networks incorporating fluid flow (gaseous and liquid), heat and mass transfer, chemical reactions, controls, etc. providing a user-friendly simulation environment for modeling simple and complex physical processes. It provides an object-oriented approach towards creating reusable component libraries and expresses the system behaviour in terms of differential-algebraic equations and discrete events. It uses "EcoDiagram" as its basic tool for creating schematic models incl. data initialization of the components and "EcoMonitor" to generate variable outputs, graphical charts, variable lists.

## II. EcosimPro S/W Kernel

EcosimPro (Ref. 6) provides a fixed directory structure where all the files required to execute it are stored along with sample files and basic libraries. The user is able to create as many directories for his specific work as he needs for storing new libraries by indication where these libraries are to be stored. This fixed directory configuration comprises the S/W tool directory and a number of subdirectories.

The working environment is similar to MS Visual Basic, C++ or other programs, which run in a MS Windows XP environment.

EcosimPro provides a library structure as a collection of components related to a specific simulation environment (thermal, hydraulic, control, rocket engine, cryogenic stage, etc.).

Figure II-1 shows the main window *EcoStudio* of EcosimPro. Here, the different components of a library can be modelled in the editor using the S/W programming language EL (EcosimPro Language). It provides all that is required to model a component or set of components in a user-friendly manner. EL also provides an API (Application Programming Interface) for standard programming languages (FORTRAN, C++).

A new library is created via a dialog box containing the identifier and the path to the directory where the library elements are stored. After giving the library an identifier, the library tree window is automatically updated and the library being created appears in the tree structure. Libraries are able to be protected.

Modelling the components which will belong to the created library is performed using the editing area. A window is opened for editing a single component(s) or a whole set of components, functions, ports, etc. After saving the library files, the library tree window is automatically updated and the library files being created appear in the tree structure.

A programming language called "EL" is provided with sequential statements similar to FORTRAN, C++ but also "continuous" and "discrete" statements to model combined continuous-discrete physical systems. It allows mathematical modelling of complex components represented by non-linear differential or algebraic equations. The

language is clear and easy to use for engineers doing such simulations and is based on an object-oriented approach: "components" inherit from one another and are able to aggregate to create more complex, modular components

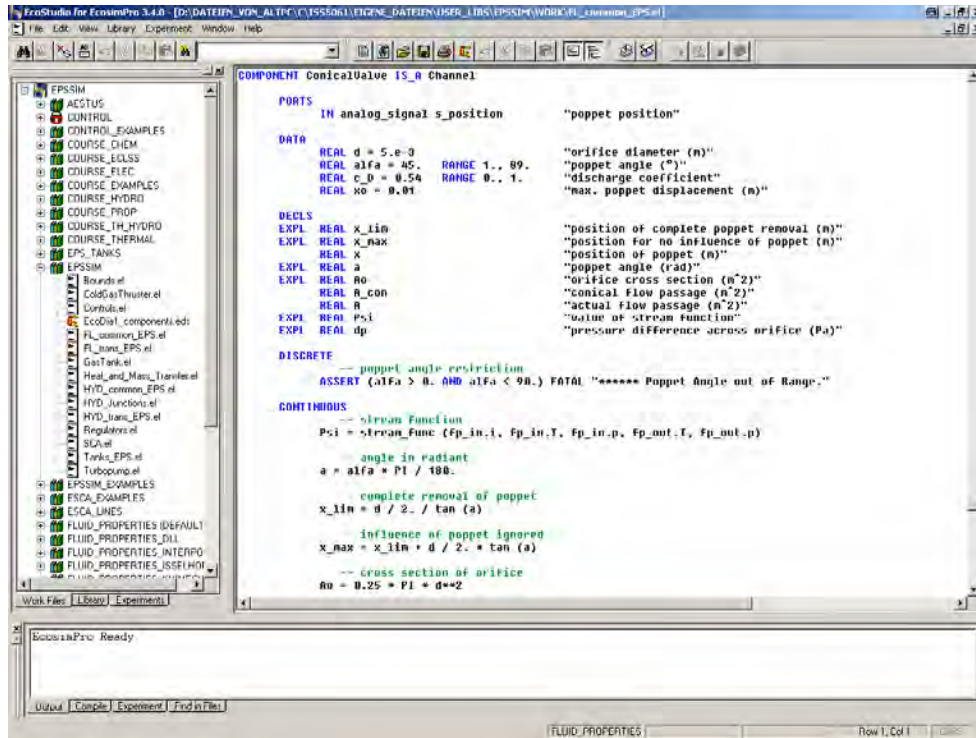


Figure II-1. EcosimPro Main Window of EcoStudio

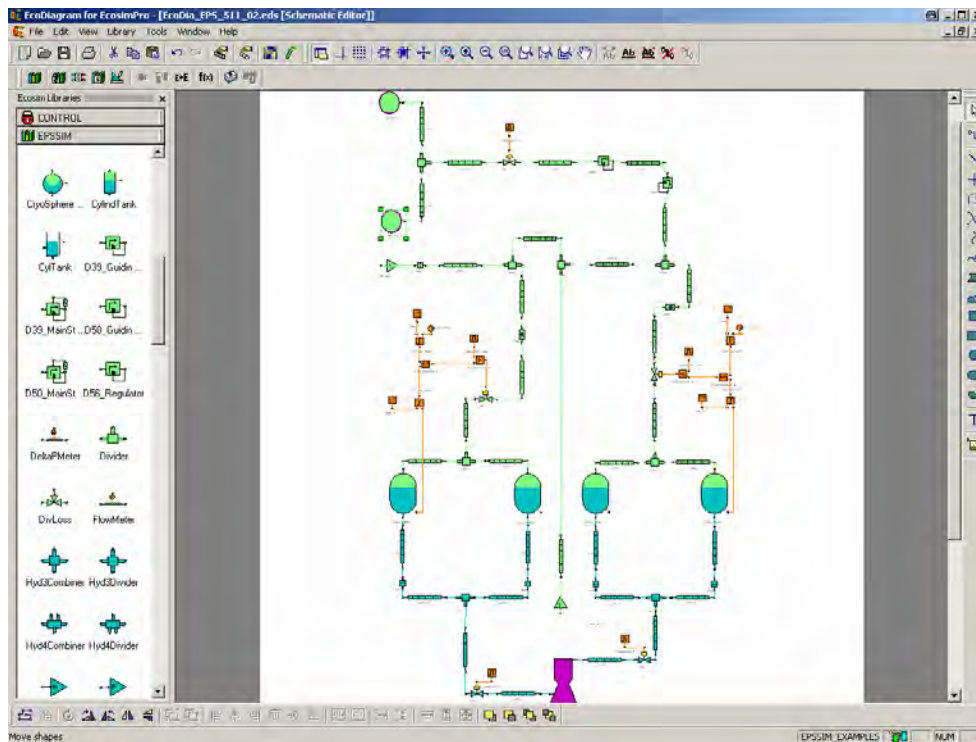


Figure II-2. EcosimPro Main Window of EcoDiagram

The key element is a "component" which is the equivalent of the "class" concept in object-oriented programming. The component represents a model by means of variables, topology, equations and event-based behaviour. All components have a block that represents the "continuous" equations and another that handles all "discrete events". "Ports" define a set of variables to be interchanged in connections of components.

Figure II-2 shows the main window *EcoDiagram* of EcosimPro which is the basic tool for creating schematic models incl. data initialization of the components. This 2D schematic diagram is able for enabling graphically complex stage models quickly and easily with the drag and drop technique. The environment is similar to popular MS Visio®. Those schematics can be created without knowledge of the modelling language. The S/W generates automatically a file with the S/W language code for further processing.

Figure II-3 shows the main window *EcoMonitor* of EcosimPro which is the basic tool to generate variable outputs, graphical charts, variable lists.

An interaction to other S/W platforms i.e. MS Excel is already available. I/F to e.g. ESATAN or Flow3D as 3D thermal or CFD (Computational Fluid Dynamics) codes, respectively, will be foreseen in enhanced versions of EcosimPro.

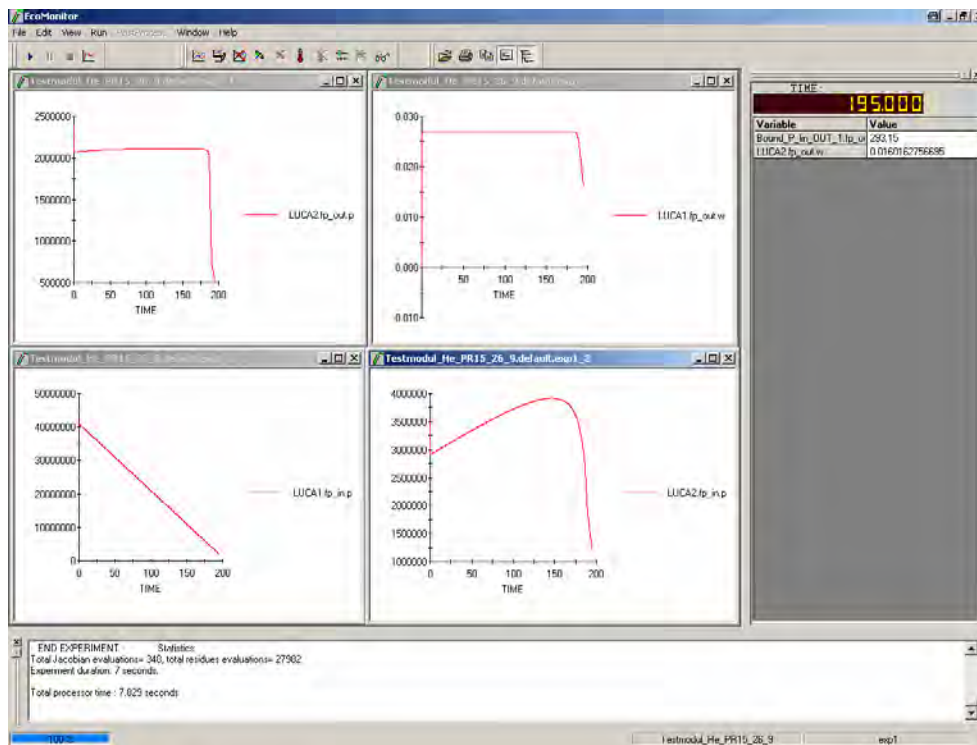
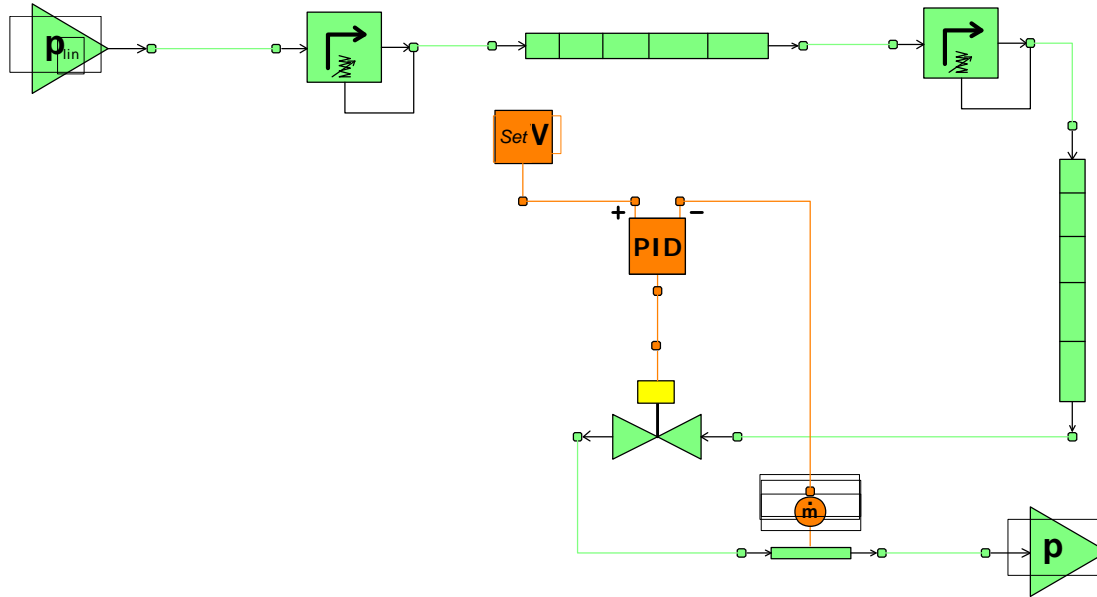


Figure II-3. EcosimPro Main Window of EcoMonitor

### III. Regulator Test Bench Model

The regulator test bench model is a simplification of the real test bench used at *Air Liquide (AL)*. It has been reduced to the main functional components to characterise and adjust the behaviour of the two regulator stages for a given "constant" mass flow rate  $\dot{m}$  to obtain the specified regulated pressure under high pressure blow-down conditions between 400 to 44 bar. The high pressure inlet boundary incorporates the time-dependent properties ( $p(t), T(t)$ ) of the high pressure Helium gas measured on the AL test set-up in front of the 1<sup>st</sup> regulator stage. The two regulator stages are each a individual **COMPONENT** with a Line **COMPONENT** as the intermediate volume. The mass flow rate  $\dot{m}(t)$  which is not really a constant value during the test is considered via a PID controlled conical valve, where the measured value on AL test bench is used as a time-dependent Set Value and the value  $\dot{m}$  of the Flow Meter **COMPONENT** as Actual Value for the PID controller **COMPONENT**. The low pressure outlet boundary is set to the environmental pressure.

On the Ariane 5 EPS stage the 2-stage pressure regulator (Ref. 5) has to reduce the high pressure level of the pressurant gas stored in two vessels to an appropriate level to expel the propellant at constant mass flow rates. The mass flow through the regulator stage orifice, separating the high pressure from the low pressure chamber, is driven by the associated high and low pressure conditions, as well as the effective orifice cross section which is dependent upon the poppet position relative to the orifice. The poppet displacement is controlled by the two different pressures acting at the poppet high and low pressure side as well as on the bellow. These forces are counteracted by the spring forces and by forces resulting from rapid poppet movements i.e. inertia and friction. For the purpose of hardware adjustment to a specified level, the pre-stress of the individual poppet/bellow spring systems must be calibrated.



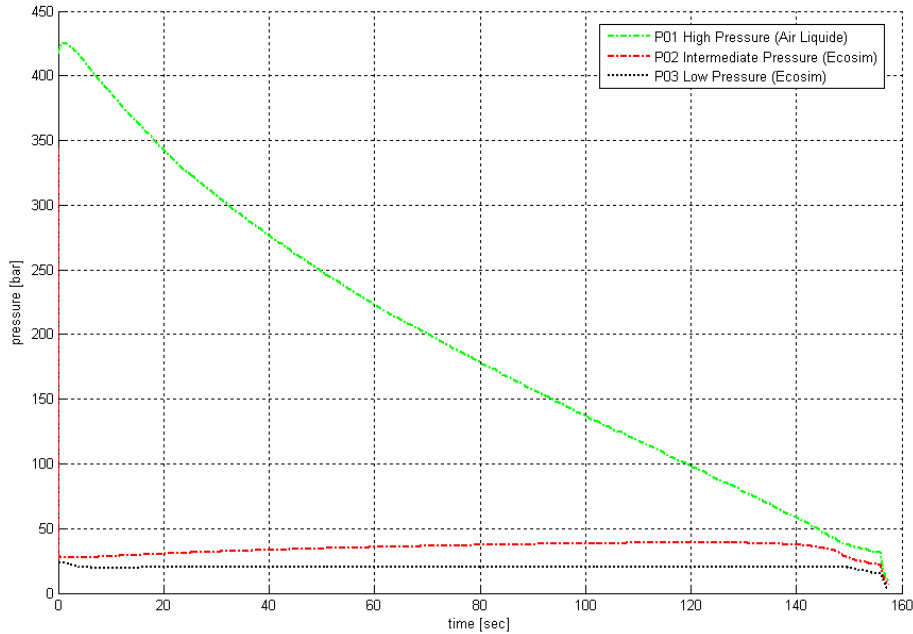
**Figure III-1: Schematic of the Regulator Test COMPONENT**

Figure III-1 shows the simplified schematic of the EPS regulator test bench for adjustment of the pre-stress load of the main spring of the two regulator stages. The **p<sub>lin</sub> COMPONENT** represents the time-dependent pressure and temperature of the feeding Helium gas taken from the acceptance data in tabulated form, the **p COMPONENT** represents the atmospheric condition. The **Set V COMPONENT** stores the corresponding mass flow rates in tabulated form taken from the AL acceptance data package. It delivers the time-dependent mass flow command value for the **PID COMPONENT** whereas the actual value of the mass flow is delivered by the **Flow Meter COMPONENT**. The PID Controller is connected to the **Conical Valve COMPONENT** which regulates the mass flow accordingly.

High Pressure Stage					Low Pressure Stage				
discharge coefficient	spring stiffness	poppet mass	viscous damping	pre-stress of spring	discharge coefficient	Spring stiffness	poppet mass	viscous damping	pre-stress of spring
c <sub>D</sub>	c <sub>sp</sub>	m	mu	F <sub>Pre</sub>	c <sub>D</sub>	c <sub>sp</sub>	m	mu	F <sub>Pre</sub>
[-]	[N/mm]	[kg]	[Pa*s]	[N]	[-]	[N/mm]	[kg]	[Pa*s]	[N]
0.65	500	0.1	5000	1050	0.60	120	0.1	2000	850

**Figure III-2: Values obtained after Adjustment to Air Liquide measured Data**

Figure III-2 shows the best fit of adjusted model parameters for the two EPS regulator stages. Figure III-3 shows the high pressure slope (400 to 44 bar) for which the regulator is specified to regulate at a mean value of  $20.77 \pm 0.15$  bar for a constant mass flow rate of 26.9 g/s and a Helium inlet temperature of 20°C. Figure III-4 shows the inlet temperature measured on the AL test bench in front of the 1<sup>st</sup> regulator stage.



**Figure III-3: High Pressure Slope of  $p_{01}$  for Regulator Test taken from Air Liquide Data (Ref. 8)**

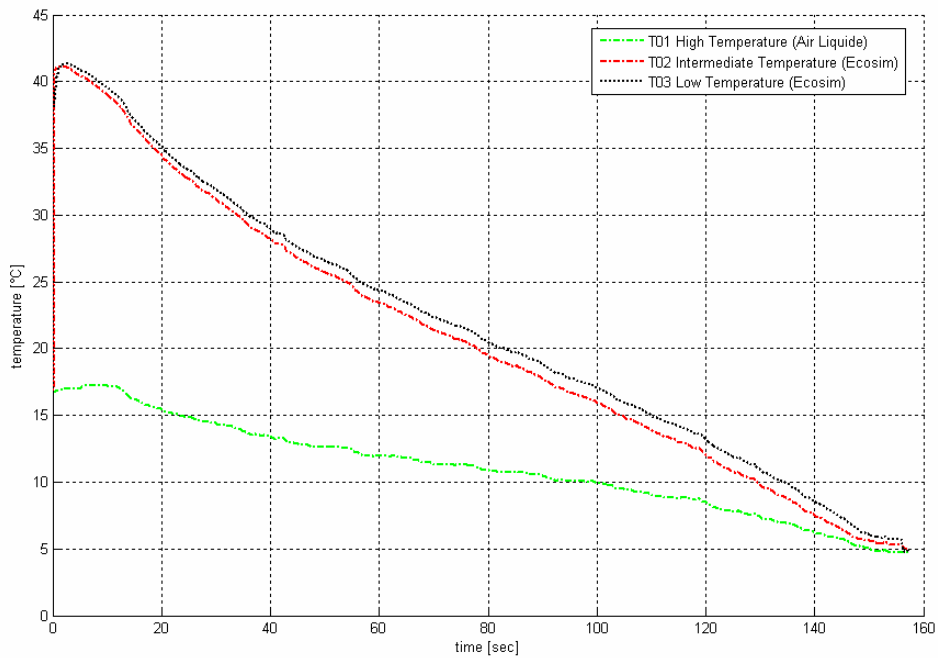


**Figure III-4: Inlet Temperature Slope of  $T_{01}$  for Regulator Test taken from Air Liquide Data (Ref. 8)**



The intermediate pressure  $p_{02}$  is specified to regulate at a mean value of  $36.0 \pm 0.8$  bar, respectively. The pressure slopes  $p_{02}$  and  $p_{03}$  acc. to Figure III-5 and the mass flow rate acc. to Figure III-6 are obtained, showing the following accordance between *EcosimPro regulator model* and *Air Liquide Acceptance Test Data (Ref. 8)*.

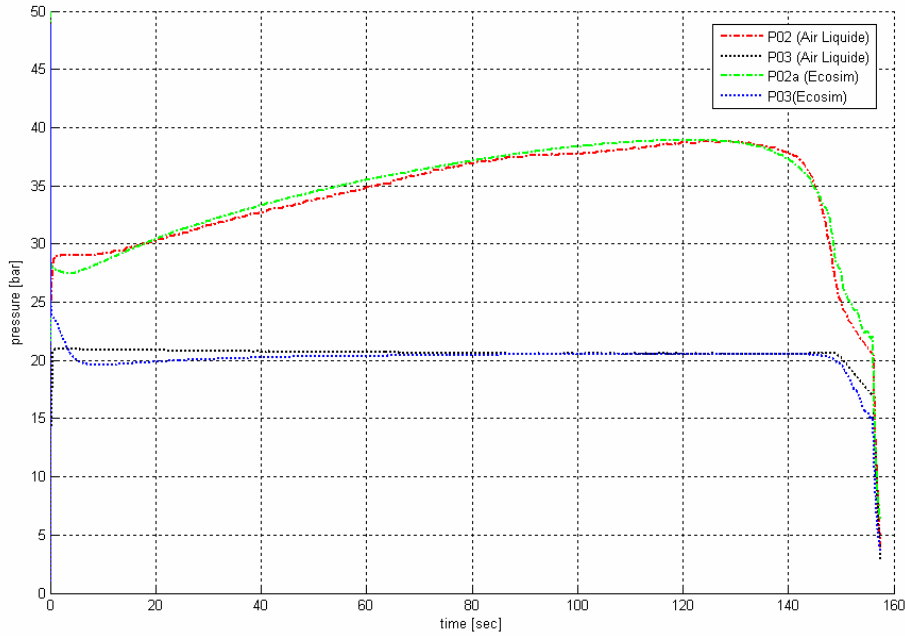


**Figure III-5: Comparison of Pressure Slopes  $p_{02}$  and  $p_{03}$  of Regulator Model with Air Liquide Data (Ref. 8)**

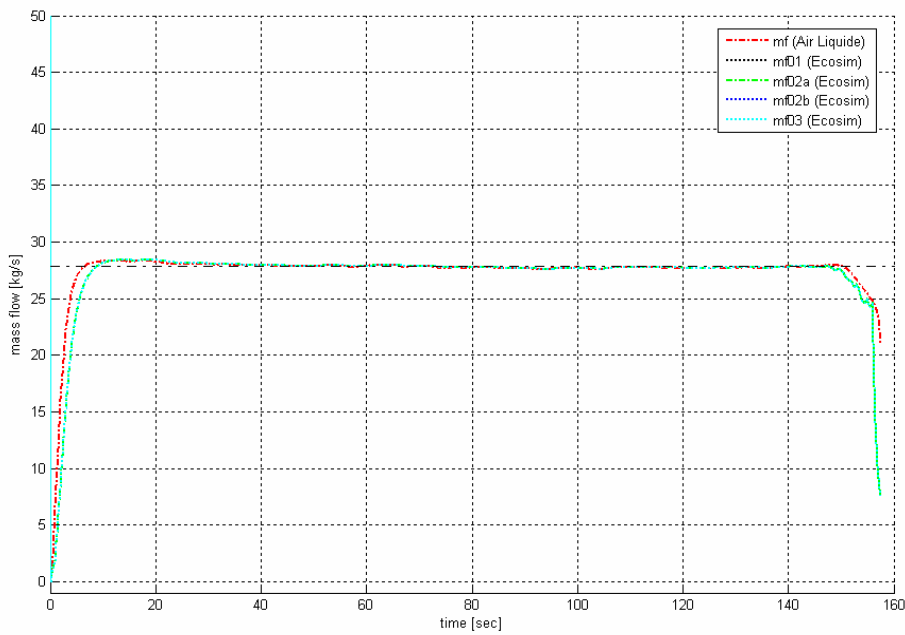


**Figure III-6: Comparison of Mass Flow Rate Slope  $\dot{m}$  of Regulator Model with Air Liquide Data (Ref. 8)**

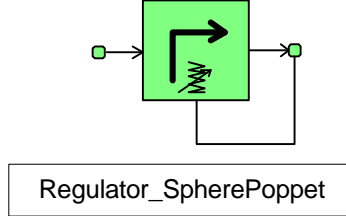


#### IV. Physical Formulation of Components

The physical formulation of the components used in the chosen simplified functional model of the acceptance test bench for the 2-stage pressure regulator of the Ariane 5 EPS upper stage is presented hereafter (Ref. 5).

##### A. Mechanical Pressure Regulator

- *Symbol:*



- *Input Wizard:*

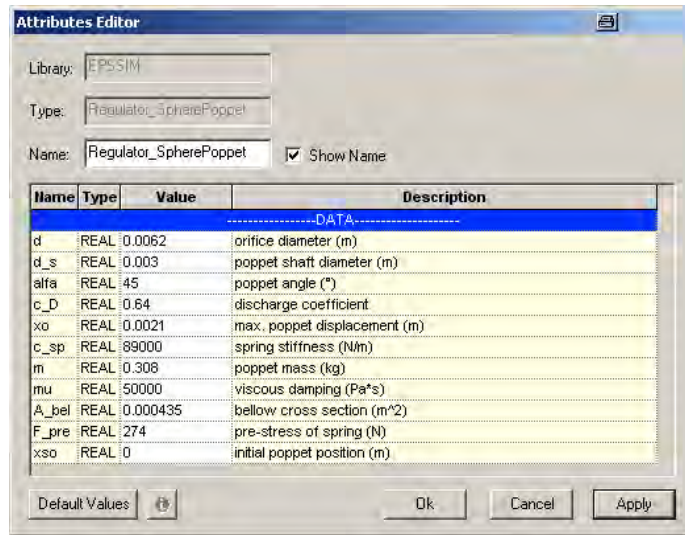


**Figure IV-1. Input Wizard of Regulator Sphere Poppet COMPONENT**

- *Formulation:*

The rapid movement of a regulator poppet during initial phases requires the consideration of mass inertia effects. According to Newton's principles the balance of the associated forces, as induced by springs, pressures and mass inertias, yields:

$$F_{pre} + F_{spring} + F_{pop,HP} + F_{pop,LP} + F_{bel} + F_{damp} + F_{inert} = 0 \quad (IV.1)$$

with the following definitions:

- $F_{pre}$  denotes the pre-load of the combined springs, which is used for regulator downstream pressures adjustment.
- $F_{spring}$  represents the spring load with decreasing poppet opening  $x < x_o$ :

$$F_{spring} = c_{sp} (x_o - x) \quad (IV.2)$$

- $F_{bel}$  denotes the pressure force acting on the bellow, which is mounted at the low pressure side of the stage:

$$F_{bel} = - A_{bel} (p_a - p_{bel,int}) \quad (IV.3)$$

$p_{bel}$  represents the bellow internal pressure, which is set to be equal to the stage ambient pressure and therefore very small compared with the magnitude of  $p_a$ .

- $F_{pop}$  denotes the forces acting on effective poppet surfaces:

$$F_{pop,HP} = - A_{pop,HP} P_i \quad (IV.4)$$

$$F_{pop,LP} = + A_{pop,LP} P_a \quad (IV.5)$$

- $F_{damp}$  represents the friction acting on the poppet movement. Damping is induced by the springs, the bellow as well as the poppet shaft, which is guided by a sleeve. According to the theory for spring/mass oscillators the

damping force is assumed to be equal to the associated velocity of the poppet movement, multiplied by a constant damping factor  $\mu_{sh}$ :

$$F_{damp} = -\mathbf{m}_{sh} \dot{x} \quad (IV.6)$$

- $F_{inert}$  denotes inertia effects due to all moveable masses of the stage:

$$F_{inert} = -\mathbf{m}_{sh} \ddot{x} \quad (IV.7)$$

Substitution and re-arrangement of equation IV.1 yields a linear differential equation of 2<sup>nd</sup> order, describing the motion of the poppet:

$$m_{sh} \ddot{x} + \mathbf{m}_{sh} \dot{x} - c_{sp} (x_o - x) = F_{pre} - A_{pop,HP} p_i - (A_{bel} - A_{pop,LP}) p_a + p_\infty A_{bel} \quad (IV.2)$$

The poppet displacement is restricted to the range of  $0 \leq x \leq x_o$ . The dynamic theory presented covers also the steady state behaviour of the regulator stage. The characteristics are only distinguished by means of inertia and damping effects. Consequently, the poppet displacement  $x$  results in:

$$x = x_o + \frac{1}{c_{sp}} (F_{pre} - A_{pop,HP} p_i - (A_{bel} - A_{pop,LP}) p_a + p_\infty A_{bel}) \quad (IV.3)$$

Steady state **lock up** conditions  $p_{lock\ up} = p_a$  can be simply derived from the above equation, with a poppet displacement equal to zero:

$$p_{lock\ up} = \frac{A_{pop,HP} p_i - F_{pre} - c_{sp} x_o - p_\infty A_{bel}}{A_{pop,LP} - A_{bel}} \quad (IV.4)$$

The mass flow rate is calculated according to the St. Venant-Wantzel equation (Ref. 1), which is based upon the rules of gas-dynamics for compressible fluids, the mass flow rate generally yields:

$$\dot{m} = c_D A(x) \Psi \sqrt{2 p_i r_i} \quad (IV.5)$$

with  $i$  and  $a$  denoting the regulator inlet and outlet conditions, respectively. For the stream function  $\Psi$  a distinction has to be introduced between sub-critical and supercritical pressure ratios. The critical pressure ratio is defined as:

$$\left( \frac{p_a}{p_i} \right)_{crit} = \left( \frac{2}{k+1} \right)^{\frac{k}{k-1}} \quad (IV.6)$$

Accordingly, the stream function yields for supercritical flow conditions

$$\Psi_{max} = \left( \frac{2}{k+1} \right)^{\frac{1}{k-1}} \sqrt{\frac{k}{k+1}} \quad (IV.7)$$

and for sub-critical flow conditions:

$$\Psi = \left\{ \frac{k}{k-1} \left[ \left( \frac{p_a}{p_i} \right)^{\frac{2}{k}} - \left( \frac{p_a}{p_i} \right)^{\frac{k+1}{k}} \right] \right\}^{\frac{1}{2}} \quad (IV.8)$$

The equation of state for ideal gases is corrected for compressibility effects at high pressure with the factor  $Z$ :

$$p = \mathbf{r} R T Z \quad (IV.9)$$

where the real gas factor  $Z$  depends on the pressure and temperature. The effective mass flow rate  $\dot{m}$  considers the following effects:

- friction by the velocity coefficient  $\mathbf{j}$ ,
- jet contraction by the contraction coefficient  $\mathbf{a}$ .

which can be combined to the discharge coefficient  $c_D$ .

$$\dot{m} = \mathbf{j} \mathbf{a} \dot{m}_{th} = c_D \dot{m}_{th} \quad (IV.10)$$

Another formation is the friction factor  $\mathbf{z}$ . The discharge coefficient  $c_D$  can be converted into the friction factor  $\mathbf{z}$ :

$$\mathbf{z} = \frac{1}{c_D^2} \quad (IV.11)$$

The variable geometrical characteristic of a spherical poppet is shown in Figure IV-2. The spherical poppet valve is given by

$$A = \mathbf{p} \cdot l \cdot \left( \frac{d}{2} + r \right) \quad (IV.12)$$

with

$$r = R \cdot \sin(\mathbf{q}) \quad (\text{IV.13})$$

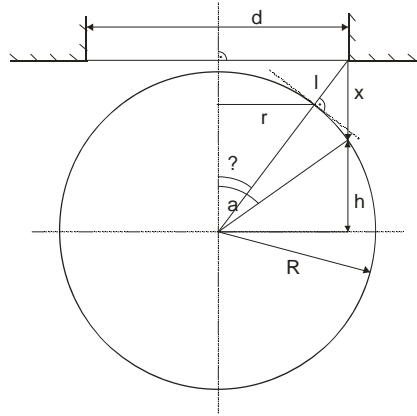


**Figure IV-2. Spherical Poppet**

From basic geometrical dependencies as shown in Figure IV-2 the length  $l$  results as follows

$$l = R \cdot \cos(\mathbf{a} - \mathbf{q}) + x \cdot \cos(\mathbf{q}) - R \quad (\text{IV.14})$$

The poppet displacement  $x$  is derived next

$$\frac{d}{2} = (h + x) \cdot \tan(\mathbf{q}) \quad (\text{IV.15})$$

$$\frac{d}{2} = h \cdot \tan(\mathbf{a}) \quad (\text{IV.16})$$

$$x = \frac{d}{2} \cdot \left( \frac{1}{\tan(\mathbf{q})} - \frac{1}{\tan(\mathbf{a})} \right) \quad (\text{IV.17})$$

Furthermore the ball radius and the orifice radius depend on each other as follows

$$\frac{d}{2} = R \cdot \sin(\mathbf{a}) \quad (\text{IV.18})$$

Equation (IV.14) to (IV.18) result in

$$l = \frac{d}{2} \cdot \frac{\cos(\mathbf{a} - \mathbf{q})}{\sin(\mathbf{a})} - \frac{d}{2} \cdot \frac{1}{\sin(\mathbf{a})} + \frac{d}{2} \cdot \cos(\mathbf{q}) \cdot \left[ \frac{\cos(\mathbf{q})}{\sin(\mathbf{q})} - \frac{\cos(\mathbf{a})}{\sin(\mathbf{a})} \right] \quad (\text{IV.19})$$

Using the general trigonometric dependency

$$\cos(\mathbf{a} - \mathbf{q}) = \cos(\mathbf{a}) \cdot \cos(\mathbf{q}) + \sin(\mathbf{a}) \cdot \sin \mathbf{q} \quad (\text{IV.20})$$

Equation (IV.19) finally results in

$$l = \frac{d}{2} \cdot \frac{\cos(\mathbf{a}) \cdot \cos(\mathbf{q})}{\sin(\mathbf{a})} + \frac{d}{2} \cdot \sin(\mathbf{q}) - \frac{d}{2} \cdot \frac{1}{\sin(\mathbf{a})} + \frac{d}{2} \cdot \cos(\mathbf{a}) \cdot \left[ \frac{\cos(\mathbf{q})}{\sin(\mathbf{q})} - \frac{\cos(\mathbf{a})}{\sin(\mathbf{a})} \right] \quad (\text{IV.21})$$

The conical flow passage given by equation (IV.12) results in

$$A = \mathbf{p} \cdot \frac{d^2}{4} \cdot \left( \frac{\cos(\mathbf{a}) \cdot \cos(\mathbf{q})}{\sin(\mathbf{a})} + \sin(\mathbf{q}) - \frac{1}{\sin(\mathbf{a})} + \cos(\mathbf{a}) \cdot \left( \frac{\cos(\mathbf{q})}{\sin(\mathbf{q})} - \frac{\cos(\mathbf{a})}{\sin(\mathbf{a})} \right) \right) \cdot \left( 1 + \frac{\sin(\mathbf{q})}{\sin(\mathbf{a})} \right) \quad (\text{IV.22})$$

Using the general trigonometric dependency

$$\sin^2(\mathbf{a}) + \cos^2(\mathbf{a}) = 1 \quad (\text{IV.23})$$

Equation (IV.22) finally results in

$$A = \mathbf{p} \cdot \frac{d^2}{4} \cdot \frac{1}{\sin(\mathbf{q})} \cdot \left( 1 - \frac{\sin^2(\mathbf{q})}{\sin^2(\mathbf{a})} \right) \quad (\text{IV.24})$$

To get numerically the flow passage in dependency of the poppet displacement the angle  $\mathbf{q}$  needs to be calculated using equation:

$$\mathbf{q} = \arctan \left( \frac{1}{\frac{1}{\tan(\mathbf{a})} + \frac{2 \cdot x}{d}} \right) \quad (\text{IV.25})$$

If the poppet opening rate is high enough, the corresponding conical flow passage may exceed the cross sectional area of the orifice. The condition for that case is given by

$$A \geq A_{\text{orifice}} = \frac{\mathbf{p}}{4} \cdot (d^2 - d_s^2) \quad (\text{IV.26})$$

This condition defines an angle  $\mathbf{q}_{\text{lim}}$ , for which a quadratic equation in  $\sin \mathbf{q}$  must be solved:

$$1 = \frac{1}{\sin(\mathbf{q}_{\text{lim}})} \cdot \left( 1 - \frac{\sin^2(\mathbf{q}_{\text{lim}})}{\sin^2(\mathbf{a})} \right) \quad (\text{IV.27})$$

The solution is of this equation is:

$$\sin(\mathbf{q}_{\text{lim}}) = -\sin^2(\mathbf{a}) + \sin(\mathbf{a}) \cdot \sqrt{1 + \frac{1}{4} \sin^2(\mathbf{a})} \quad (\text{IV.28})$$

$x \geq x_{\text{lim}}$  defines the case of a complete removal of the poppet.

$$x_{\text{lim}} = \frac{d}{2} \cdot \left( \frac{1}{\tan(\mathbf{q}_{\text{lim}})} - \frac{1}{\tan(\mathbf{a})} \right) \quad (\text{IV.29})$$

Figure IV-3 shows the cross-sections in dependency of the ratio of the poppet displacement to the orifice diameter for different ratios of radii  $\frac{R}{R_k}$ .

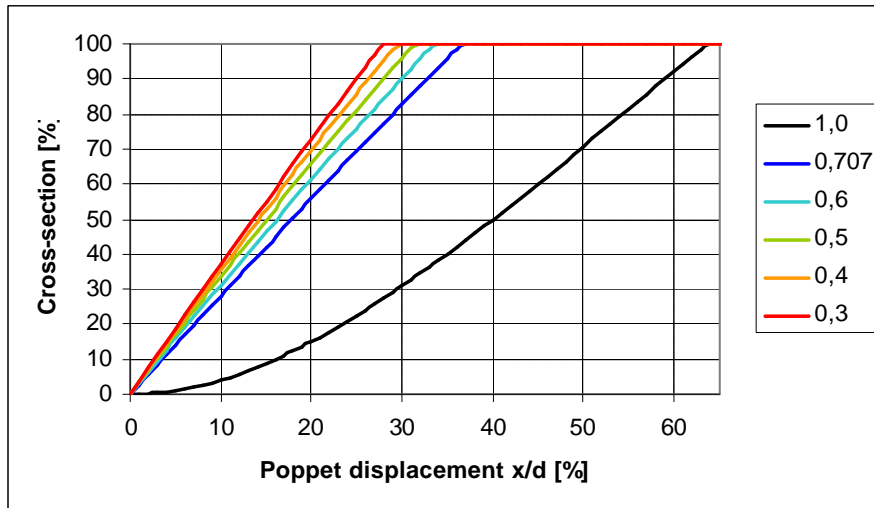
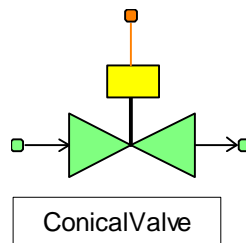


Figure IV-3. Cross-Sections of the Spherical Poppet Valve

## B. Conical Valve

- *Symbol:*



- *Input Wizard:*

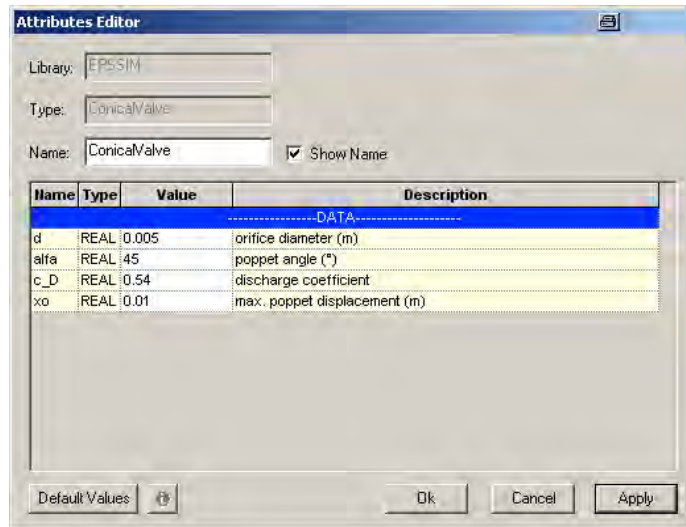


**Figure IV-4: Input Wizard of Conical Valve COMPONENT**

- *Formulation:*

The geometrical characteristic of a conical valve is described as shown in Figure IV-5.

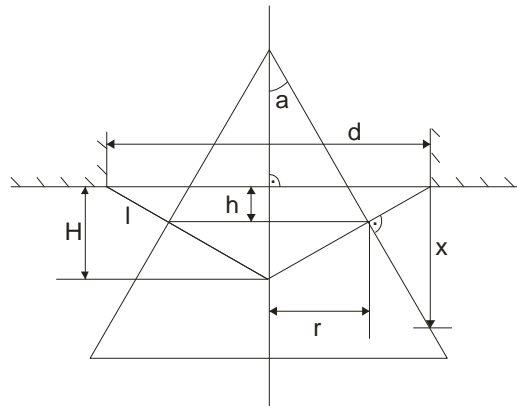


**Figure IV-5: Conical Valve**

The cross-section is derived in dependency of the poppet displacement.

$$l = x \cdot \sin(\mathbf{a}) \quad (\text{IV.30})$$

$$h = l \cdot \sin(\mathbf{a}) = x \cdot \sin^2(\mathbf{a}) \quad (\text{IV.31})$$

The total height of the upside down cone is given by

$$H = h + \frac{h \cdot r}{R - r} \quad (\text{IV.32})$$

With the given orifice diameter the radius results in

$$R = \frac{d}{2} \quad (\text{IV.33})$$

$$H = R \cdot \tan(\mathbf{a}) \quad (\text{IV.34})$$

The combination of equation (IV.32) and (IV.34) results in

$$R \cdot \tan(\mathbf{a}) = h + \frac{h \cdot r}{R - r} \quad (\text{IV.35})$$

From equation (IV.35) the second radius of the truncated cone can be derived

$$r = R - x \cdot \sin(\mathbf{a}) \cdot \cos(\mathbf{a}) \quad (\text{IV.36})$$

The conical flow passage is then given by

$$A = \mathbf{p} \cdot l \cdot (R + r) \quad (\text{IV.37})$$

and finally results in

$$A = \mathbf{p} \cdot x \cdot \sin(\mathbf{a}) \cdot (d - x \cdot \sin(\mathbf{a}) \cdot \cos(\mathbf{a})) \quad (\text{IV.38})$$

If the poppet opening rate is high enough, the corresponding conical flow passage may exceed the cross sectional area of the orifice. The condition for that case is given by

$$A \geq A_{\text{orifice}} = \mathbf{p} \cdot R^2 \quad (\text{IV.39})$$

$x \geq x_{\text{lim}}$  defines the case of a complete removal of the poppet.

$$x_{\text{lim}} = \frac{d}{2 \cdot \tan(\mathbf{a})} = \frac{R}{\tan(\mathbf{a})} \quad (\text{IV.40})$$

The influence of the poppet can be ignored if the displacement exceeds  $x_{\text{max}}$ , see Figure IV-6.

$$x_{\text{max}} = x_{\text{lim}} + H = x_{\text{lim}} + R \cdot \tan(\mathbf{a}) \quad (\text{IV.41})$$

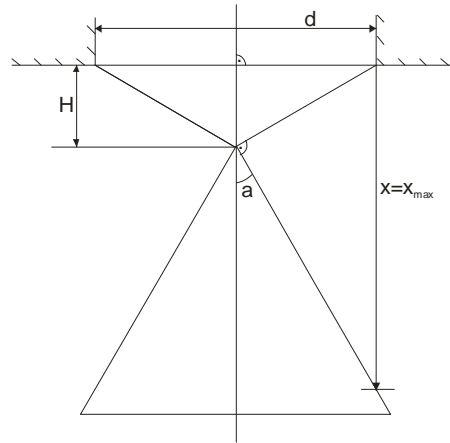


Figure IV-6: Maximum Displacement of Poppet

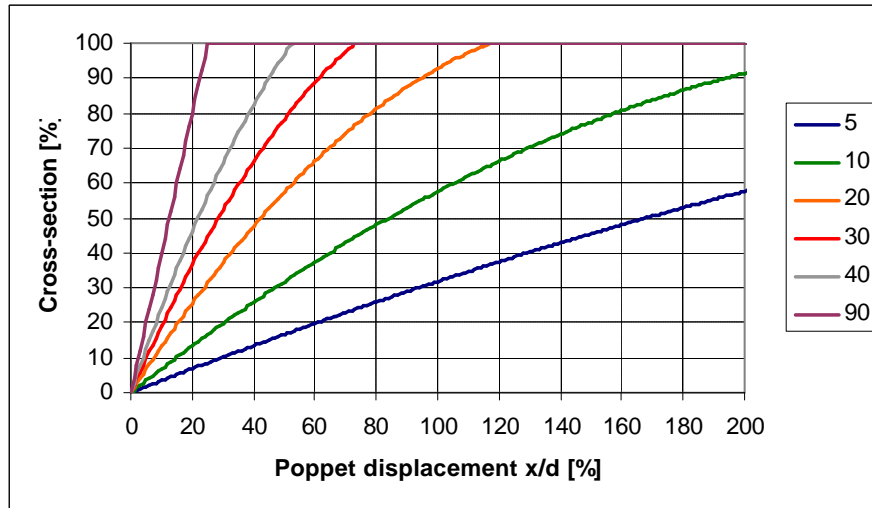
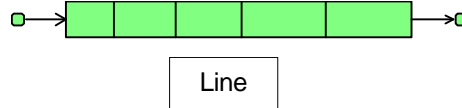


Figure IV-7: Cross-Sections of Conical Valve

Figure IV-7 shows the cross-sections in dependency of the ratio of the poppet displacement to the orifice diameter for different poppet angles  $\alpha$ .

### C. Pneumatic Line Section

- *Symbol:*



- ? *Input Wizard:*

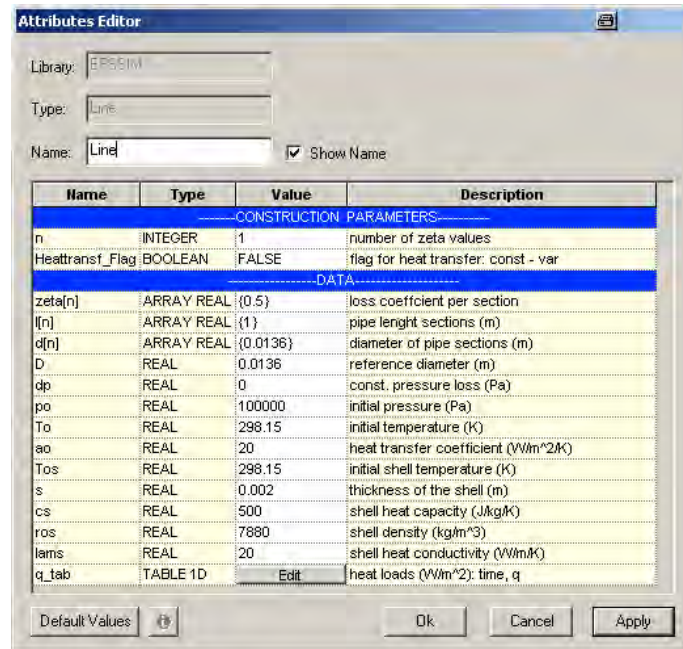


Figure IV-8: Input Wizard of Line COMPONENT

- *Formulation:*

The Line COMPONENT will be a single component gas volume considered with expansion and compression physics by mass, momentum and energy conservation. Mass, enthalpy and pressure at in- and outlet as well as momentum loss due to friction within the pipe is encountered under steady (without time derivative of the momentum equation) conditions. It is used to represent a pipe section e.g. between two junctions. A reference loss coefficient related to a reference diameter is calculated by an array of constant loss pressure loss coefficients whereas each is related to a specific pipe diameter to account for specific pipe elements of the considered pipe section. A connection to a solid surrounding wall is performed by heat transfer coefficient represented by Nusselt theory or constant value.

The solid wall is composed of a solid conducting volume. Only the cylindrical shape is actually considered. Heat transfer to the environment is defined by time-dependent data table consisting of heat loads W/m<sup>2</sup>.

The formulation of the heat transfer within the gas volume is derived from the fundamental equations of fluid dynamics i.e. conservation of mass and energy. The conservation of momentum is implicitly included in the dimensionless quantities (Pr, Re, Gr, Ar, Ra). The state in the bulk of the pipes is characterized in a time-dependent mode.

The application of *pressure* and *temperature* as state variables requires the availability of the partial derivatives of density with respect to pressure and temperature.

- ? *Conservation of mass:*

The rate of change of mass  $m$  in each control volume is given by:



$$\frac{dm}{dt} = \dot{m}_{in} - \dot{m}_{out} \quad (\text{IV.42})$$

The change of density in each control volume can be calculated from the time derivative of  $m = \rho V$  :

$$\dot{\rho} V = \dot{m} \quad (\text{IV.43})$$

The derivative of the density can be calculated from the derivatives of the temperature and pressure:

$$\frac{d\rho}{dt} = \left. \frac{\partial \rho}{\partial p} \right|_T \cdot \frac{dp}{dt} + \left. \frac{\partial \rho}{\partial T} \right|_p \cdot \frac{dT}{dt} \quad (\text{IV.44})$$

? *Conservation of momentum:*

The equation of conservation of momentum is applied in the steady state formulation for the inlet and outlet mass flow rates, respectively:

$$p_{in} - p = V_D \cdot \frac{\dot{m}_{in}^2}{4\rho A_D^2} \quad (\text{IV.45})$$

$$p - p_{out} = V_D \cdot \frac{\dot{m}_{out}^2}{4\rho A_D^2} \quad (\text{IV.46})$$

? *Conservation of energy:*

The equation of conservation of energy is:

$$\frac{dE}{dt} = \dot{m}_{in} \cdot h_{in} - \dot{m}_{out} \cdot h_{out} + \dot{Q} \quad (\text{IV.47})$$

The total energy in the control volume can be expressed  $E = m e$  .

Taking into account that  $e = u + \frac{1}{2} v^2$  ,  $u = h - \frac{p}{\rho}$  and neglecting the influence of the velocity:

$$m\dot{h} + \dot{m}h - \dot{p}V = \dot{m}_{in} \cdot h_{in} - \dot{m}_{out} \cdot h_{out} + \dot{Q} \quad (\text{IV.48})$$

But an additional equation has to be introduced. The derivative of the specific enthalpy can be calculated from the derivatives of the temperature and pressure:

$$\frac{dh}{dt} = \left. \frac{\partial h}{\partial p} \right|_T \cdot \frac{dp}{dt} + \left. \frac{\partial h}{\partial T} \right|_p \cdot \frac{dT}{dt} \quad (\text{IV.49})$$

The derivative of the specific enthalpy to the temperature at constant pressure is obtained by:

$$\left. \frac{\partial h}{\partial T} \right|_p = c_p \quad (\text{IV.50})$$

The derivative of the specific enthalpy to the pressure at constant temperature is obtained by:

$$\left. \frac{\partial h}{\partial T} \right|_T = v - T \cdot \left. \frac{\partial v}{\partial T} \right|_p \quad (\text{IV.51})$$

The isobaric expansion coefficient  $\beta$  is defined as:

$$\left. \frac{\partial v}{\partial T} \right|_p = \beta v \quad (\text{IV.52})$$

Introduction of the isobaric expansion coefficient  $\beta$  and the specific heat capacity  $c_p$  results in:

$$dh = c_p dT + v(1 - \beta T) dp \quad (\text{IV.53})$$

? *Friction loss coefficients:*

The presentation of loss coefficient data is made using circular cross-section pipes elements of constant area. Loss coefficients vary remarkable with Re number and, usually to a lesser extend, with inlet and outlet pipe arrangements and with surface roughness. Basic loss coefficients are defined at a Re number of  $10^6$  with long and hydraulically smooth inlet and outlet pipes or passages. Correction factors are given to correct to any Re number and outlet or passage length. Generally, loss coefficients are a function of pipe diameter, relative radius of curvature, the relative roughness and the bend angle (Ref. 3).

In our case loss coefficients  $V_i$  are given in form of a data string for the  $i$  sections for which additionally, the respective diameter  $d_i$  and length  $l_i$  has to be defined from which the cross section  $A_i$  is derived:

$$A_i = \frac{\mathbf{p}}{4} d_i^2 \quad (\text{IV.54})$$

The reference values are expressed for the total pipe length as:

$$L = \sum_{i=1}^n l_i \quad (\text{IV.55})$$

for the flow channel surface:

$$S = \mathbf{p} \cdot \sum_{i=1}^n l_i d_i \quad (\text{IV.56})$$

and for the flow channel volume:

$$V = \sum_{i=1}^n l_i A_i \quad (\text{IV.57})$$

The overall reference pressure loss coefficient  $V_D$  is:

$$V_D = A_D^2 \cdot \sum_{i=1}^n \frac{V_i}{A_i^2} \quad (\text{IV.58})$$

with

$$A_D = \frac{\mathbf{p}}{4} d_D^2 \quad (\text{IV.59})$$

? *Convective heat transfer:*

The considered phenomena of the heat and mass transfer are described. The expected phenomena inside a propellant or pressurant pipe are especially related to the upper stages currently in production within the Ariane 5 program. In practice, the heat transfer at the pipe wall is important. Considering a wall with the temperature  $J_w$  and a fluid with the bulk temperature  $J$  (not the temperature inside the boundary layer) moving along the wall the resulting heat flux density is proportional to the difference of both temperatures.

$$\dot{q}_w = -\mathbf{a} (J - J_w) \quad (\text{IV.60})$$

The proportionality factor  $\mathbf{a}$  is defined as heat transfer coefficient.

Close to the wall where the fluid has no velocity the energy can only be transported by conduction. Therefore, the heat flux density at the wall can be derived with by

$$\mathbf{a} = -l \frac{\left( \frac{\partial J}{\partial y} \right)}{J - J_w} \quad (\text{IV.61})$$

For the determination of the heat transfer coefficient the temperature field needs to be known which requires the exact knowledge of the velocity field. In most realistic cases the heat transfer coefficients need to be evaluated by experimental results.

The phenomenon of forced convection can be divided into two parts which is relevant for pipe flow. On the one side, the region of laminar convection flow exists where the conservation equations are valid and solvable for simple cases. In the second region with turbulent flow, the heat transfer in the boundary layer is increased by the turbulent fluctuation motion of the fluid and additional assumptions have to be considered for solving the conservation equations.

The averaged heat transfer coefficient  $\mathbf{a}$  along the pipe length  $l$  is defined by:

$$\dot{q}_w = -\mathbf{a} \Delta J_{\log} \quad (\text{IV.62})$$

The value  $\Delta J_{\log}$  is the logarithmic temperature difference (Ref. 4):

$$\Delta J_{\log} = \frac{(J_w - J_e) \cdot (J_w - J_a)}{\ln \frac{J_w - J_e}{J_w - J_a}} \quad (\text{IV.63})$$

? *laminar forced convection:*

The temperature and velocity profiles developed from the pipe entrance are called the hydrodynamic and thermal start-up. The length of this region can be estimated by considering that the boundary layer thickness is half of the pipe diameter which results in:

$$L_a = 0.02 \cdot \text{Re} \cdot d \quad (\text{IV.64})$$

For hydrodynamic laminar flow conditions the relation according to *Hausen* is valid for gases and liquids (Ref. 4):

$$Nu_{lam} = \left( 3.66 + \frac{0.19 \left( \text{Re} \text{Pr} \frac{d}{l} \right)^{0.8}}{1 + 0.117 \left( \text{Re} \text{Pr} \frac{d}{l} \right)^{0.467}} \right) \quad (\text{IV.65})$$

With very low deviations the dependence is given by following equation from *Schlünder* (Ref. 4):

$$Nu_{lam} = \sqrt[3]{3.66^3 + 1.61^3 \text{Re} \text{Pr} \frac{d}{l}} \quad (\text{IV.66})$$

with the Re number:

$$\text{Re} < 2300 \quad (\text{IV.67})$$

The presented equations are valid for gases and liquids in the range of:

$$0.1 < \text{Re} \text{Pr} \frac{d}{l} < 10^4 \quad (\text{IV.68})$$

Fluid properties are to be used at the averaged temperature  $J_m$ :

$$J_m = \frac{J_e + J_a}{2} \quad (\text{IV.69})$$

and the Pr number influence for liquids via the viscosity difference between wall  $J_w$  and averaged fluid temperature  $J_m$ :

$$f = \left( \frac{\text{Pr}}{\text{Pr}_w} \right)^{0.11} \quad (\text{IV.70})$$

? *turbulent forced convection:*

For hydrodynamic turbulent flow conditions the relation according to *Gnielinsky* is valid for gases and liquids (Ref. 4):

$$Nu_{turb} = \frac{\frac{x}{8} (\text{Re} - 1000) \text{Pr}}{1 + 12.7 \sqrt{\frac{x}{8}} \cdot \left( \text{Pr}^{\frac{2}{3}} - 1 \right)} \cdot \left( 1 + \left( \frac{d_i}{l} \right)^{\frac{2}{3}} \right) \quad (\text{IV.71})$$

with the pressure loss coefficient to be used according to *Filonenko* (Ref. 4):

$$x = (1.82 \log_{10} \text{Re} - 1.64)^{-2} \quad (\text{IV.72})$$

For smooth pipes the pressure loss coefficient can be expressed with little deviations by the following:

$$x = \frac{0.188}{\text{Re}^{0.2}} \quad (\text{IV.73})$$

with the Re number:

$$8000 < \text{Re} < 3 \cdot 10^6 \quad (\text{IV.74})$$

For the heat transfer it is now obtained (Ref. 4):

$$Nu_{turb} = \frac{0.0235 \text{Re}^{0.8} \text{Pr}}{1 + 1.947 \text{Re}^{-0.1} (\text{Pr}^{0.667} - 1)} \quad (\text{IV.75})$$

Similar to the flow along a plain plate this equation can be simplified, if the Prandtl number influence is summarized to a simple power expression:

$$Nu_{turb} = 0.0235 \cdot \text{Re}^{0.8} \text{Pr}^{0.48} \quad (\text{IV.76})$$

with the Re and Pr number ranges:

$$10^4 < \text{Re} < 10^6; \quad 0.6 < \text{Pr} < 50 \quad (\text{IV.77})$$

Fluid properties are to be used at the averaged temperature  $\mathbf{J}_m$  :

$$\mathbf{J}_m = \frac{\mathbf{J}_e + \mathbf{J}_a}{2} \quad (\text{IV.78})$$

and the Pr number influence for liquids via the viscosity difference between wall  $\mathbf{J}_w$  and averaged fluid temperature  $\mathbf{J}_m$  :

$$f = \left( \frac{\text{Pr}}{\text{Pr}_w} \right)^{0.11} \quad (\text{IV.79})$$

To account for hydrodynamic and thermal inlet flow conditions which are  $l \approx 27 \cdot d$  for  $\text{Re} = 10^5$  is expressed by:

$$f = \left( 1 + \left( \frac{d}{l} \right)^{\frac{2}{3}} \right) \quad (\text{IV.80})$$

? *pipe wall:*

The cylindrical shell of pipe elements is considered as a 2D formulation in cylindrical coordinates for evaluating the temperature distribution in direction of the shell thickness and length. The wall thickness of such pipes is in the range of several millimetres and the length in the range of meters. The pipes are often made of stainless steel.

The shell is divided into a number of sub-layers for solving the heat equation as a function of thickness  $s$  and length  $l$  and time  $t$ . Convection heat transfer on the inner and outer surface is used as time-dependent boundary condition for the time-dependent behaviour. The relevant energy equation for the 2D shell model can be written in the following form:

$$\mathbf{r}_s c_s \frac{\partial T_s}{\partial t} = \frac{l}{r} \frac{\partial}{\partial r} \left( r \mathbf{I}_s \frac{\partial T_s}{\partial r} \right) \quad (\text{IV.81})$$

An essential point is that in the radial derivative  $dr$  should not simply be replaced by  $\Delta r$  due to the increase of the shell surface  $S = 2\pi r L$  with increasing radius  $r$ . The term  $r dT/dr$  has therefore to be replaced by the equivalent term  $dT/d(\ln r)$ , so that the energy equation is in the form:

$$\int_V \mathbf{r}_s c_s \frac{\partial T_s}{\partial t} dV = \int_V \frac{l}{r} \frac{\partial}{\partial r} \left( \mathbf{I}_s \frac{\partial T_s}{\partial \ln r} \right) dV \quad (\text{IV.82})$$

In the formulation for the pipe shell, the integral formulation of the heat equation is used. Additionally, the volume integral of the divergence of the heat flux  $\nabla \vec{q}$  is transferred into a surface integral of the heat flux  $\vec{q}$  with the help of the Gaussian divergence theorem.

The heat flux  $\dot{Q}$  leads to the following equation between wall and fluid:

$$\dot{Q} = - \frac{S}{\frac{1}{a} + \frac{r \cdot \ln \left( \frac{r_s}{r} \right)}{l}} \cdot (T - T_s) \quad (\text{IV.83})$$

For the shell internal energy  $u$  follows therefore:

$$\frac{du_s}{dt} \cdot V_s = - \dot{Q} + \dot{Q}_s \quad (\text{IV.84})$$

with

$$V_s = \pi r_s^2 L - V \quad (\text{IV.85})$$

The derivative of the shell temperature  $\dot{T}_s$  is calculated from:

$$\dot{u}_s = \mathbf{r}_s c_s \dot{T}_s \quad (\text{IV.86})$$

The external heat load can be differently applied. One method is to give time-dependent heat loads in a data table or via a function:

$$\dot{Q}_s = S_s \cdot q(t) \quad (\text{IV.87})$$

with

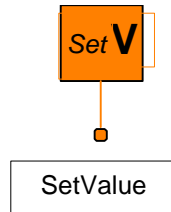
$$S_s = 2pr_s L \tag{IV.88}$$

Another way to define heat loads is to deliver a data table where

$$\dot{Q}_s = S_s \cdot q(T_\infty - T_s) \tag{IV.89}$$

**D. Set Value**

- *Symbol:*



- *Input Table*

- *Input Wizard:*

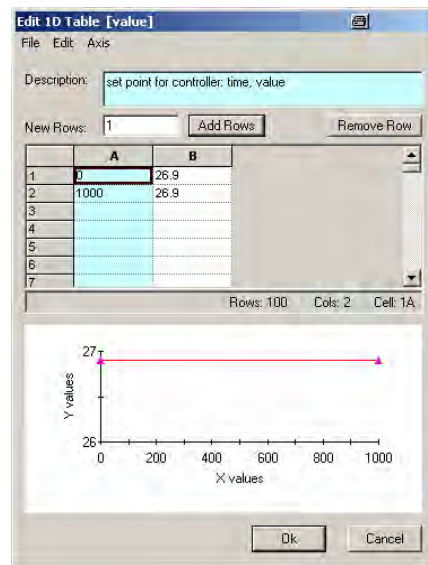
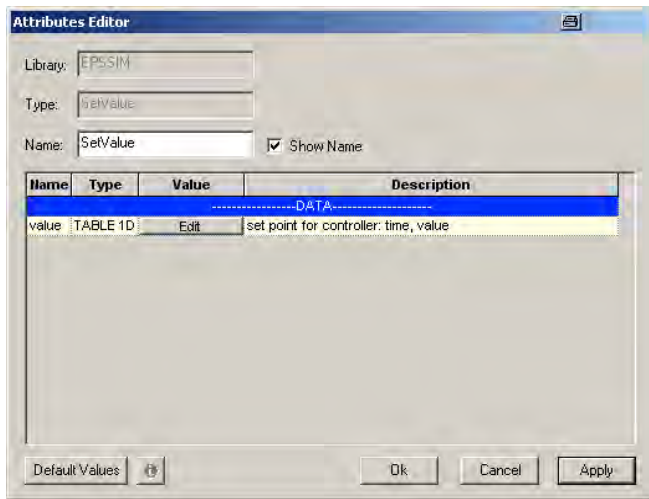


**Figure IV-9: Input Wizard of Set Value COMPONENT**

**Figure IV-10: Input Table of Set Value COMPONENT**

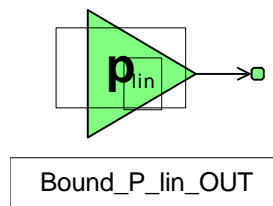
- *Formulation:*

The value  $v$  of this COMPONENT is fixed as a boundary condition:

$$s_{out} = v(t) \tag{IV.90}$$

**E. Bound P lin OUT**

- *Symbol:*



- *Input Wizard:*

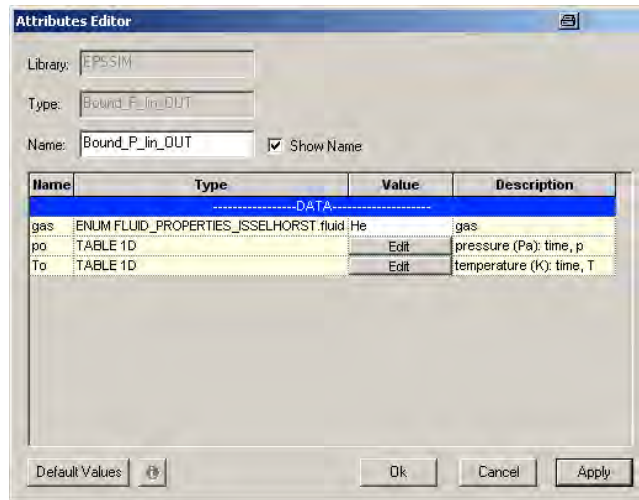


**Figure IV-11: Input Wizard of Bound P lin OUT COMPONENT**

- *Formulation:*

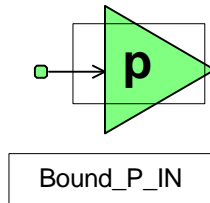
The pressure and temperature in the **PORT COMPONENT** is fixed as a boundary condition:

$$p_{out} = p(t) \tag{IV.91}$$

$$T_{out} = T(t) \tag{IV.92}$$

**F. Bound P IN**

- *Symbol:*



- *Input Wizard:*

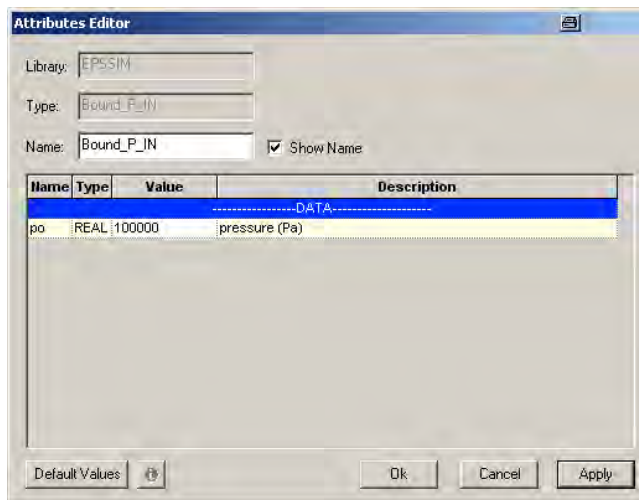


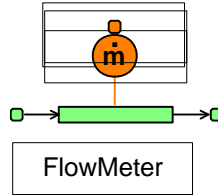
**Figure IV-12: Input Wizard of Bound P IN COMPONENT**

- *Formulation:*  
The pressure in the **PORT COMPONENT** is fixed as a boundary condition:

$$p_{in} = p \tag{IV.93}$$

### G. Flow Meter

- *Symbol:*



- *Input Wizard:*

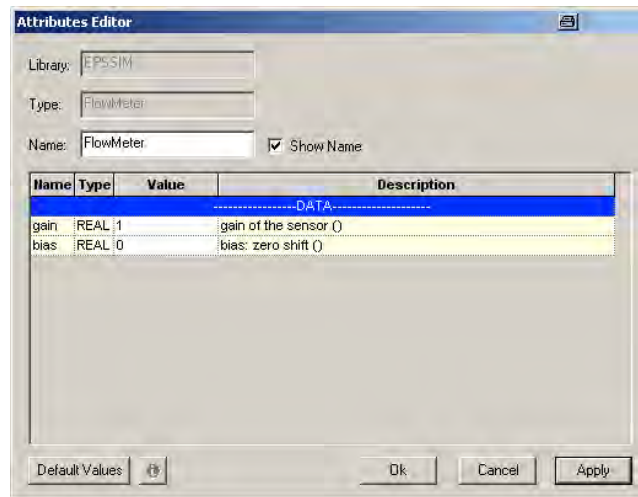


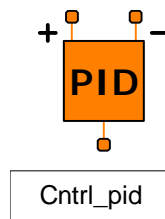
**Figure IV-13: Input Wizard of Flow Meter COMPONENT**

- *Formulation:*  
The value of the measured variable  $v$  is equal to the mass flow rate in the **PORT**:

$$v = \dot{m} \tag{IV.94}$$

### H. PID Controller

- *Symbol:*





- *Input Wizard:*

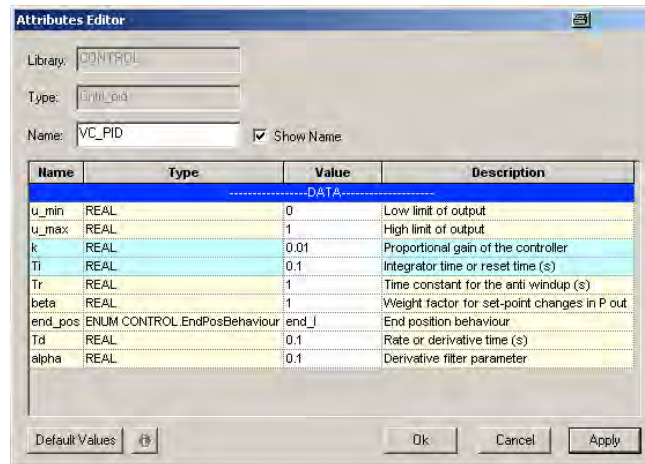


Figure IV-14: Input Wizard of PID Controller COMPONENT

- *Formulation:*

The PID Controller is a standard COMPONENT delivered with the EcosimPro S/W. The formulation is presented in Ref. 6.

## V. Conclusion

The regulator test bench model shows the as a 1<sup>st</sup> example the power and possibilities of EcosimPro object-oriented S/W approach. A well adjusted set of model parameters for the Ariane 5 EPS regulator could also be achieved w.r.t. the acceptance data delivered by AL. The next step will be to set up a full EPS functional stage model and to perform flight analysis simulations and to compare those to Ariane 5 EPS flight measurement data. For the new cryogenic upper stage ESC-A the relevant COMPONENTS will be developed next to build up the stage model.

## Acknowledgments

The **euces** project Part I was funded by BMBF (federal ministry of education and science) with account no. 50JR0503 and was performed at EDAS-ST GmbH.

## References

### Books

- <sup>1</sup>Bohl, W.; *Technische Strömungslehre*, 9<sup>th</sup> ed., Vogel Buchverlag, Würzburg, 1991, pp. 206, 217.
- <sup>2</sup>Stephan, K.; Mayinger, F.; *Thermodynamik Band 1, Einstoffsysteme. Grundlagen und technische Anwendungen*, 14<sup>th</sup> ed., Springer-Verlag, Heidelberg/Berlin, 1992, pp. 17, 152.
- <sup>3</sup>Miller, D.S.; *Internal Flow Systems*, 2<sup>nd</sup> ed., Unwin Brothers Ltd., 1990
- <sup>4</sup>VDI-Gesellschaft Verfahrenstechnik und Chemieingenieurwesen; *VDI-Wärmeatlas*, 8<sup>th</sup> ed., Springer-Verlag, Berlin Heidelberg, 1997

### Reports, Theses, and Individual Papers

- <sup>5</sup>Isselhorst, A.; **euces**, *Simulation of Launcher Propulsion Systems, Study on numerical Modeling and Simulation of Launcher Stages for propelled and non-propelled Flight Phases*, Final Report Part I, EADS-ST **euces**-RIBRE-FR-0001, 2006.

### Computer Software

- <sup>6</sup>EcosimPro; *A Professional Dynamic Modeling and Simulation Tool for Industrial Applications*, Ver. 3.4, EAI Empresarios Agrupados International, Madrid, Spain, 2005.

### EADS-ST internal Documents

- <sup>7</sup>C<sup>3</sup>B-RIBRE-TN-0007-DASA (1), *Analysis of Commercial and in-house Simulation S/W*
- <sup>8</sup>A5-CE-192224-X-2002-AIRL (1), *EPS Pressure Regulator / PR15 Acceptance Test Minute*